1st Latin-American Workshop on Structural Health Monitoring
LATAM-SHM 2023
December, 5-8 2023

IN-SITU STRAIN MEASUREMENT OF CONCRETE MICRO-PILES UNDER LOADING USING DISTRIBUTED FIBER OPTIC SENSING SYSTEMS

MARIO TERCEROS*, WALTER PANIAGUA†, FRANCISCO j. CARRION, JORGE a. HERNANDEZ, JUAN a. QUINTANA, LUIS A. MARTÍNEZ, HÉCTOR M. GASCA+ ALEXIS MENDEZ++

* Incotec S.A.,
Av. 4to Anillo, Edif. Torre Link Piso 3, Santa Cruz, Bolivia
e-mail: math@incotec.cc

† Pilotec S.A. de C.V.
Periférico Sur 4302-106, Mexico City, Mexico 04500
e-mail: wpaniagua@pilotec.com.mx

+ Instituto Mexicano del Transporte (IMT)
Carretera El Colorado - Galindo Km. 12 Col. San Fandila, Queretaro, Mexico
e-mail: carrion@imt.mx

++ MCH Engineering, LLC
1217 Sherman St., Alameda, CA 94501, USA
e-mail: alexis.mendez@mchengineering.com (contact author)

Key Words: SHM, Structural Health Monitoring, Pile, Fiber Optic Sensing, Sensors

Abstract. We present experimental results on the measurement, in-situ and in real time, of the internal strain distribution along the height of a set of six separate micropiles with different configurations (Simple, with Expander Body and with Bidirectional Cell) using three separate fiber optic sensing techniques—two of them based on distributed Brillouin and Rayleigh scattering, and the third one based on the use of discrete fiber Bragg grating (FBG) strain sensors. The distributed techniques relied on the use of embedded fiber optic strain-sensing cables, while the FBG technique used discrete strain sensors packaged for concrete embedment. Single-point and distributed strain measurements were made during the concrete pouring and curing process, as well as post-cure under compression loading. Results showed that it is practical and possible to obtain high spatial resolution strain profiles during the diverse construction phases of the micro-piles. There was good agreement among all 3 methods in terms of the overall strain accuracy. The best results were achieved using the high resolution, Rayleigh scattering based, ODiSI instrument which has millimeter resolution strain profiles that resulted in very fine strain profiles along the concrete pile surface and the surrounding soil.

1. INTRODUCTION

Monitoring of the performance of micropiles has been an area of increased interest and research over the past decade, due to its demonstrated capability to evaluate a soil's load transfer characteristics along the length of the pile and its overall load capacity, over long periods and under different loading conditions [1]. Initially, the strain monitoring of the piles was based on VW (vibrating wire) strain gages, but more recently, optical Fiber Bragg Grating (FBG) sensors [2] and distributed fiber optic sensors (DFOS) [3,4] have being used because of their immunity to EM interference and capability to perform multi-point and distributed measurements. This work presents the measurement results form a monitoring study where DFOS were used to measure and compare the performance of three different designs of micropiles under controlled load conditions. The different designs were:

a) Simple micropile
b) Micropile with bidirectional cell on the tip
c) Micropile with expander body on the tip

Additionally, the micropile with bidirectional cell was instrumented with strain and temperature FBG sensors to monitor the concrete curing process over time.

2. INSTRUMENTATION

Two different DFOS instruments were used. The first one is based on measuring distributed strain via Rayleigh backscatter (Luna ODiSI 6104) used in combination with distributed-sensing fiber cable (Epsilon from NerveSensors). a composite DFOS sensor with strain range up to 4% and elasticity of 3 GPa, well suited for SHM of concrete elements with high sensitivity and resolution (Epsilon, 2023) under tension and compression loads, manufactured to fit needs and surface roughness to achieve perfect adhesion with concrete when embedded, with negligible sensor influence. Figure 1 shows a typical DFOS EpsilonSensor [5].

Figure 1: Epsilon Sensor DFOS

The second instrument uses Brillouin scattering to perform distributed measurements of both strain and temperature (LIOS EN.SURE). This unit was connected to a FO cable cable from NanZee Sensing. The cable consists of a single-mode fiber optic core, tightly wound within a spiral of six braided steel cables, then wrapped in a tight polyurethane outer sheath. As opposed to thermal cable, it is necessary for strain cable to have a tightly bonded design to

ensure that applied strain to the exterior sheath is transferred in a predictable and linear manner through the intermediate layers into the central fiber optic core (Figure 2).

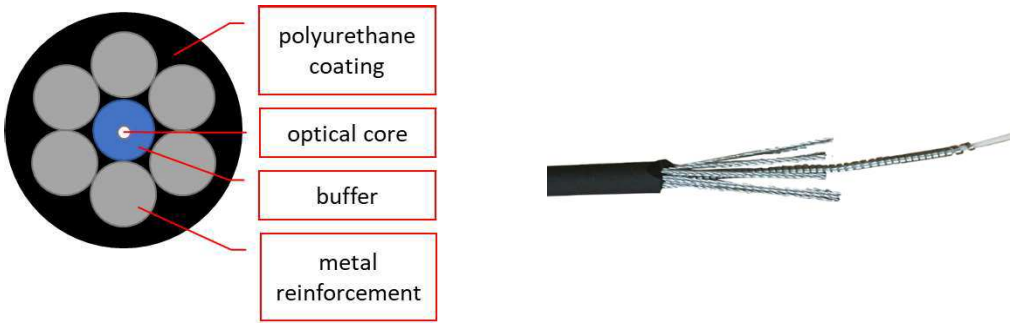

Figure 2: Schematic cross section and image of the NZS-DSS 5 mm strain cable

Discrete strain measurements were made using a Micron Optics sm130 interrogator, connected to FBG strain (ES-03 from Sylex), FBG temperature ones (Micron Optics os4350 sensors).

3. MICROPILES LOAD TESTS

Six load tests (three compression, and three tension) were carried out on the three micropiles described above. In this work, only the compression tests are reported. The test site is in Naucalpan de Juárez, State of Mexico, which is part of the project "IIUNAM Test Field, for the study of thermal properties and energy cells" [9].

3.1. Geotechnical information

The exploration campaign consisted of carrying out two standard penetration surveys at a depth of 25 m. Based on these surveys, the main geotechnical units are distinguished, described below:

- Fills (0.0m to 0.60m): On the surface, there is a fill approximately 60cm thick, made up mainly of construction material, coarse sand and brown silt.
- UG-A (0.60m a 13.0m). Below the fills, a stratum made up of medium-silty grayish-brown sand is recognized.
- UG-B (13.0m a 25.23m): Underlying the UG-A, medium to coarse grayish brown sand with little silty and strongly cemented.

3.2. Compression load tests

Compression load tests were carried out on each of the 6.50 m deep and 0.3 m diameter micropiles. The micropiles were assembled with four #6 rods and #2 stirrups, injected with water-cement grout in a 1:2 ratio (by weight). One injection stage was applied to the simple micropile (S), and two injection stages were applied to the expander body (EB) and bidirectional cell (BD) micropiles. The details of the construction procedure of each micropile can be consulted in Paniagua (2017), [10].

The reaction loads were taken with 80 cm diameter foundation piles 11.50 m deep, reinforced with reinforcing steel, using an arrangement of two reaction piles for each test micropile. In order to program the maximum loads in each load test, analytical calculations were carried out to determine the ultimate load, for each micropile condition. The detailed calculation for each type of micropile is outside the scope of this work. Table 6 shows the maximum programmed loads for each type of micropile.

Table 6: Programmed loads for load tests.

Type	Condition test	Pile diameter (m)	Max programmed load (t)	N° of reaction piles
S	Compresión	0.30	126	2
EB			144	2
BD			152	2

The compression loading test was performed using the ASTM rapid loading procedure [11]: *Procedure A*: *Quick Test*, which allows defining the ultimate load that each micropile could support, applying the load in small increments at constant time intervals. The idea is to define, as precisely as possible, the load-displacement curve of each test. In this case, the load application was chosen based on load increments in constant time intervals equivalent to 5% of the maximum load, which were applied in constant intervals of 15 min, taking the reading of all the instruments, in each increment, at 2, 5, 10, 12 and 15 minutes; Subsequently, the maximum charge was maintained for at least 1 hour, and 1 hour in the last decrement to record elastic recovery of the unloaded pile (figure 8).

For the BD micropile case, besides the two DFOS sensors (*ODiSI and LIOS*), two pairs of FBG sensors were installed, for strain and temperature measurements each pair, located at -2.75 m and -5.75 m depth, approximately (figure 8).

Figure 9 shows the floor view of the compression load test configuration; At the vertices of the triangular arrangement, reaction piles were built and the micropiles to be tested were built on the sides of the triangle. A view of one of the load test arrangements is shown in Figure 10; The reaction beam stands out, as well as the reference frame, for the installation of displacement measuring instruments at the head of the micropiles. In this same figure, the concrete heads are distinguished, both in the reaction piles and in the test micropile. Likewise, the hydraulic cylinders and pump for applying the load are shown, as well as the load cells.

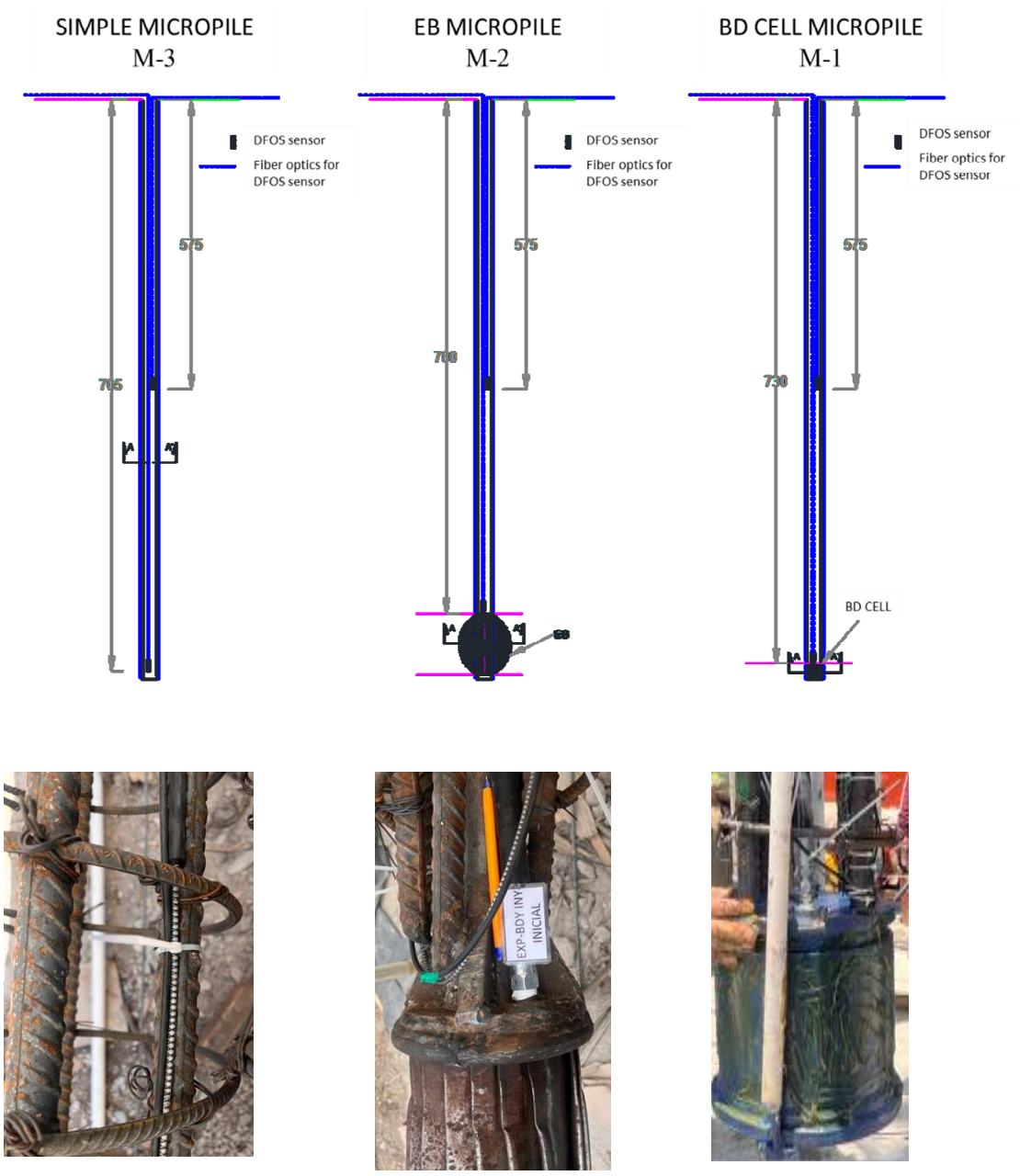

Figure 8: DFOS micropiles instrumentation.

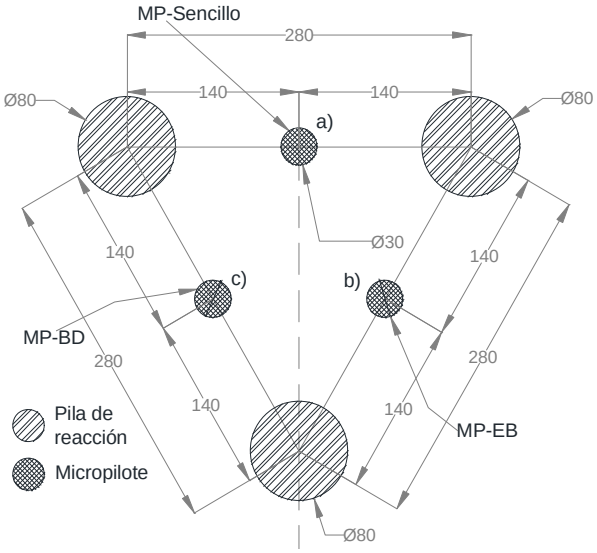

Figure 9: Diagram of micropiles and reaction piles arrangement. a) simple micropile, b) micropile with e*xpander body* y c) micropile with bidirectional cell

Figure 10: Arrangement for compression load test

3.3. Instrumentation program

Instrumentation was planned considering two different types of measurements:

a) Fiber optics instrumentation
b) Mechanical strain gages (tell-tales)

Along the length of the micropile, embedded fiber optic instruments DFOS (Distributed fiber optic sensors) and mechanical strain gauges (tell-tales) were placed on two levels at different depths. Tell-tales were placed in the simple micropile (M-3 S), and in the micropile with bidirectional cell (M-1 BD), although it was not possible to place one of these in the

micropile with expander body (M-2 EB). Table 7 shows the instrumentation program with cables and embedded fiber optic sensors and mechanical strain gauges.

Table 7: Instrumentation location in micropiles

Micropile	Level	DFOS codification	Ubicación DFOS	Ubicación Tell-tales
Simple (M-3)	1	DFOS-1	-5.75 m	-3.45 m
	2	DFOS-2	-7.05 m	-6.60 m
EB (M-2)	1	DFOS-3	-5.75 m	-
	2	DFOS-4	-7.80 m	-
BD Cell (M-1)	1	DFOS-5	-5.75 m	-3.45 m
	2	DFOS-6	-7.30 m	-6.60 m

Figure 11 shows an example of fiber optic cable placement, in this case, in the M-2 EB micropile. Figure 12 shows how a tell-tale was installed.

Figure 11: Embedded DFOS placement.

Figure 12: Placement of tell-tales in micropiles

3.4. Fiber optics instrumentation

The fiber optic instrumentation system consisted of two cables: LIOS and ODiSI, both traveling along the entire length of the micropiles, changing direction and returning within the micropile assembly. Only the micropile with a bidirectional BD cell was instrumented with FBG type sensors (see Figure 13) to measure microdeformations and temperature. Table 8 indicates the types and placement of fiber optic instrumentation.

Table 8: FO instrumentation

Interrogator	M-1 BD	M-2 EB	M-3 S
LIOS EN.SURE	(1) δ sensor (DFOS)	(1) δ sensor (DFOS)	(1) δ sensor (DFOS)
ODiSI 6104	(1) sensor δ (DFOS)	(1) sensor δ (DFOS)	(1) sensor δ (DFOS)
Micron Optics	(2) δ (FBG) (3) temperature (FBG)	-----	-----

3.5. Records during the micropile construction process.

3.5.1. Microstrain measurement

The unitary strains (microstrains) of the micropiles were recorded before casting, during casting-setting, and during grout injection (in the cases of micropiles BD and EB). Once the body of the micropile was built, a primary injection was carried out in the EB micropile to expand the chamber and subsequently, a secondary injection in the lower part. A secondary grout was injected into the BD micropile to expand the cell and generate a tip and friction preload.

Figure 13: Strain and temperature FBG instrumentation

Deformations were recorded during injections. In Figure 14 shows the readings during the application of the primary and secondary grout in the EB micropile, while Figure 15 shows the readings for the BD micropile.

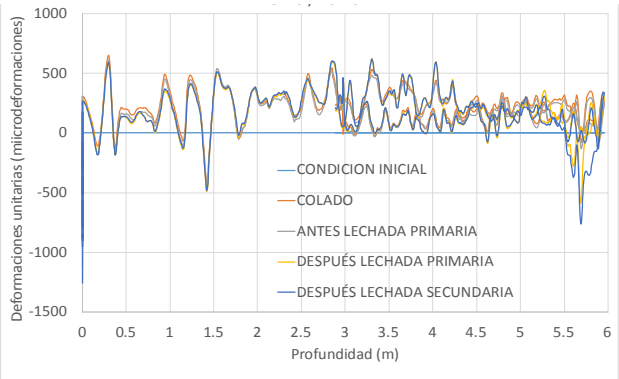

Figure 14: Microdeformations vs. depth during casting and injection, EB micropile, ODiSI cable

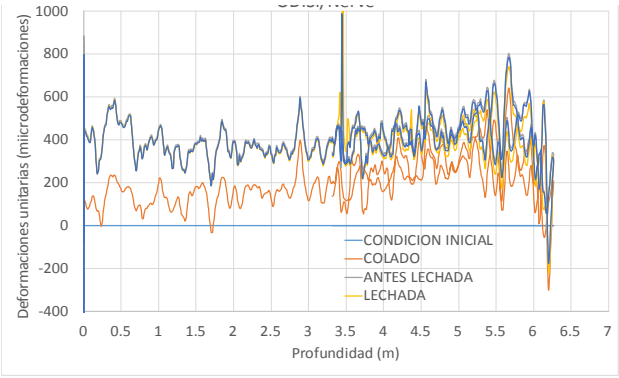

Figure 15: Microdeformations vs. depth during casting and injection, BD micropile, ODiSI cable

3.5.2. Temperature sensing

Additionally, the internal temperature was recorded during the casting-setting process at specific points of the micropile with a bidirectional cell, in the sections -0.55 m, -2.93 m and -5.79 m with the FBG sensors. Figure 16 shows the temperature curves recorded during the first hours of concrete setting.

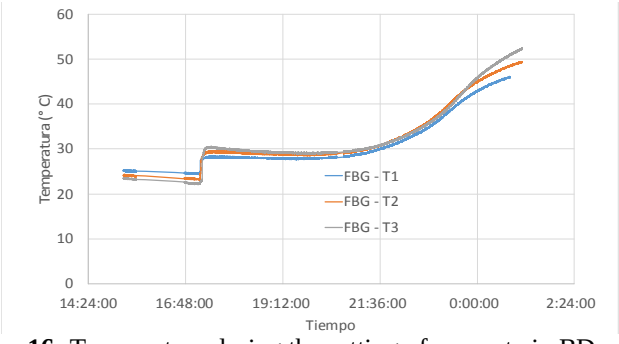

Figure 16: Temperature during the setting of concrete in BD micropile

3.6. Load test data

Figure 17 shows the load-displacement curves for the three compression load tests on micropiles M-1, M-2 and M-3.

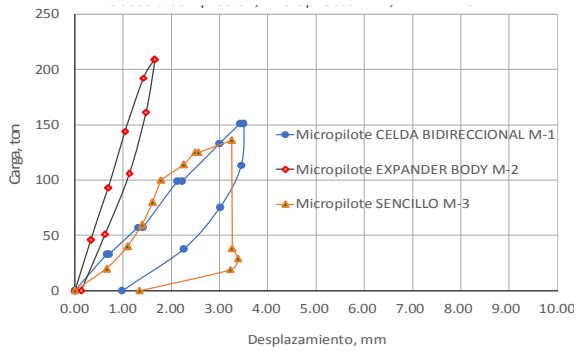

Figure 17: Load-displacement curves during compression test

Figures 18 and 19 present, as an example, the records obtained with the DFOS-NanZee and DFOS-Nerve fiber optic cables, respectively, for micropile S.

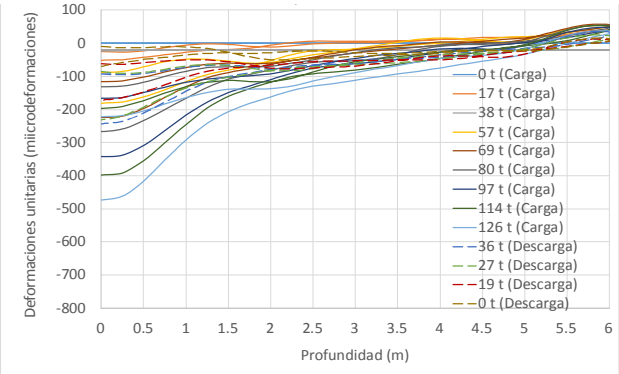

Figure 18. Microstrain vs. depth, micropile S, Brillouin DFOS cable

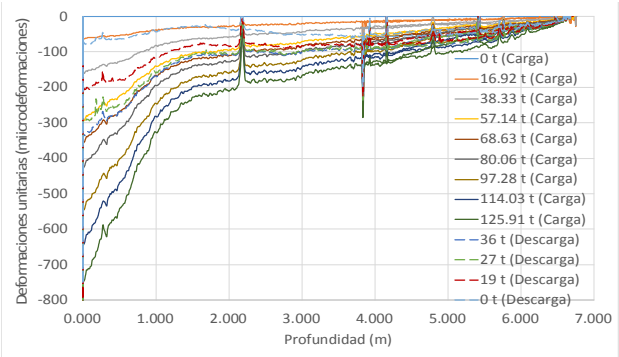

Figure 9: Microstrain vs. depth, micropile S, Raleigh scattering DFOS cable

The previous figures were obtained from the data post-processing and analysis to get the transfer curves using the incremental stiffness method [12].

Figure 20 presents the load transfer-depth curves for the S micropile (a), for BD micropile (b) and EB micropile (c); these results were obtained from the Nerve DFOS-ODiSI system and processed using the incremental stiffness modulus method.

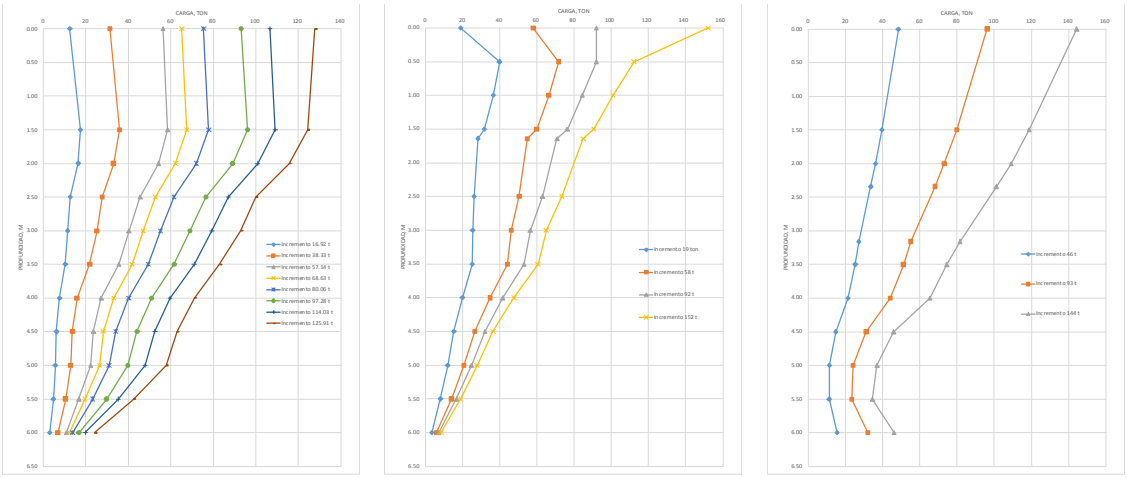

(a) Simple Micropile (b) BD Micropile (c) EB Micropile

Figure 20: Load transfer curves vs. depth, micropile S, DFOS-ODISi/Nerve cable,

3.6.1. FBG strain Sensors

Figure 21 shows the measurements obtained with the FBG sensor (Sm130-Sylex), in which the deformations detected with the sensors located in two different sections of the M-1 micropile, with a bidirectional cell, are observed. The data were obtained by graphing the unit deformation detected in the two levels of the FBG sensor vs the time of application of the loads according to the loading cycle carried out during the compression loading test.

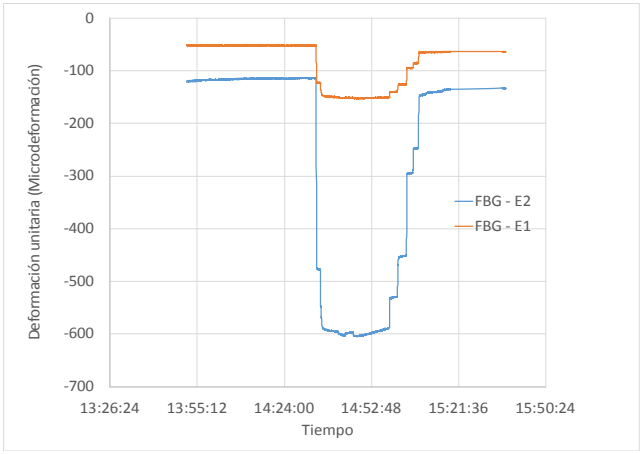

Figure 23: Microstrains *vs.* time, compression test, FBG strain sensors.

4. CONCLUSIONS

The study of three micropiles on which load tests were carried out in Mexico City, each with different design characteristics and construction procedures: simple (S), with bidirectional cell (BD) and with expander body (EB). All three were instrumented with fiber optic cables (DFOS-LIOS/Nanzee and DFOS-ODISi/Nerve) to measure microdeformations during the construction procedure and during the compression loading process. In addition to the fiber optic cabling, two FBG Sylex sensors (measurement of microdeformations in two sections) and Micron Optics (temperature measurement in three sections) were added to the BD, as well as two mechanical deformity meters in two sections (tell-tales). To micropile S, two tell-tales were added, in two sections close to the tip and close to the upper middle part of the micropile.

From the results obtained, the microdeformation profile is observed in the entire section of the micropiles with FOS cables, in each of the loading stages to which they were subjected during the compression tests, verifying their effectiveness in obtaining detailed and precise information on its internal behavior, such as microdeformations along the entire length of the element and also, occasionally, microdeformations in certain sections and temperature in the same sections during the setting of the concrete. The usefulness of fiber optic instrumentation is quite good with respect to conventional instrumentation, the main advantage being the visualization of the behavior of charge transfer with depth, practically throughout the entire length of the cable embedded in the micropile.

REFERENCES

[1] Luna, R., Dixon, D. T., Kershaw, K. A., & Siegel, T. C. (2015). Monitoring micropile foundations of bridge during construction. In IFCEE 2015 (pp. 878-889).

[2] Tsang, C. F., Mehdizadeh, A., & Disfani, M. (2020). Fibre Bragg grating sensor: a powerful technique for monitoring soil and driven mini piles interaction. In 16th Asian regional conference on soil mechanics and geotechnical engineering, ARC.

[3] Mohamad, H., Tee, B. P., Beddelee, A. A. A. M., Khoo, C. M., Ghazali, M. F., & Nasir, M. Y. M. (2023). Innovations in Micropile Testing Using Distributed Optical Fibre Sensors. In IOP Conference Series: Earth and Environmental Science (Vol. 1249, No. 1, p. 012033). IOP Publishing.

[4] Breuer S, Kammann F, Macherey R, Czerniuk T, Hill W, Komlossy K., and Kindler A. (2019) Distributed strain monitoring of reinforced concrete foundations piles during load tests. Proceedings of the 9th International Conference on Structural health Monitoring of Intelligent Infrastructure, St. Louis, MO, USA, August 4-7.

[5] Epsilon (2023). DFOS sensors. Brochure. Nerve-sensors.com.

[6] LIOS EN.SURE (2023). Distributed Structure Monitoring System. Brochure. Luna.

[7] ODiSI (2023). ODiSI 6000 Series. Optical Distributed Sensor Interrogators. Brochure

[8] SM-130 (2023) Micro Optics SM-130. Optical Sensing Interrogator sm130. Brochure. Micron Optics.

[9] Paniagua, W. (2023). Determinación de la capacidad de carga por fricción y punta de pilas de cimentación con celda de carga bidireccional en suelos granulares, Tesis de Doctorado UNAM, Ciudad de México.

[10] Paniagua, W. (2017). Micropilotes, Capítulo 7, Ingeniería de Cimentaciones Profundas. Sociedad Mexicana de Ingeniería Geotécnica, Ciudad de México.

[11] ASTM D-1143 (2007). Standard Test Methods for Deep Foundations Under Static Axial Compressive Load. ASTM International, West Conshohocken, PA, USA.

[12] Komurka, V. E., & Moghaddam, R. B. *The Incremental Rigidity Method—More Direct Conversion of Strain to Internal Force in an Instrumented Static Loading Test*. In Geo-Congress 2020 (pp. 124-134).